An Overview of Near-Field Antenna Measurements

ARTHUR D. YAGHJIAN, SENIOR MEMBER, IEEE

Abstract—**After a brief history of near-field antenna measurements with and without probe correction, the theory of near-field antenna measurements is outlined beginning with ideal probes scanning on arbitrary surfaces and ending with arbitrary probes scanning on planar, cylindrical, and spherical surfaces. Probe correction is introduced for all three measurement geometries as a slight modification to the ideal probe expressions. Sampling theorems are applied to determine the required data-point spacing, and efficient computational methods along with their computer run times are discussed. The major sources of experimental error defining the accuracy of typical planar near-field measurement facilities are reviewed, and present limitations of planar, cylindrical, and spherical near-field scanning are identified.**

I. Brief History of Near-Field Scanning

THE DEVELOPMENT OF near-field scanning as a method for measuring antennas can be divided conveniently into four periods: the early experimental period with no probe correction (1950–1961), the period of the first probe-corrected theories (1961–1975), the period in which the first theories were put into practice (1965–1975), and the period of technology transfer (1975–1985) in which 50 or more near-field scanners were built throughout the world.

A. Early Experimental Period: No Probe Correction (1950–1961)

Probably the first near-field antenna scanner was the "automatic antenna wave front plotter" built around 1950 by Barrett and Barnes [1] of the Air Force Cambridge Research Center. Although they made no attempt to compute far-field patterns from their measured near-field data, Barrett and Barnes obtained full-size maps of the phase and amplitude variations in front of microwave antennas. (A plot of the phase and amplitude contours measured in front of a 10-wavelength reflector antenna with the Barrett and Barnes wavefront plotter is shown in [2, fig. 17.5].) Woonton measured the near fields of diffracting apertures and critically examined in his 1953 paper [3] the assumption that the voltage induced in the probe is a measure of the electric field strength. Richmond and Tice [4], [5] in 1955 experimented with air and dielectric-filled, open-ended rectangular waveguide probes for measuring the near fields of microwave antennas, and compared calculated far fields with directly measured far fields. For an X-band cheese aerial, Kyle (1958) [6] compared the far-field pattern obtained directly on a far-field range with the far-field pattern computed from the near-field amplitude and phase as measured by an open-ended circular waveguide. Gamara (1960) [85] compared directly measured far-field patterns with patterns computed from amplitude and phase data taken in the near field of three different line sources excited at X-band frequencies. Good agreement was obtained over the main beams and first sidelobes of the line sources. In 1961 Clayton, Hollis, and Teegardin [7], [8] computed the principal far-field E-plane pattern for a 14-wavelength diameter reflector antenna from the amplitude and phase of the near-field distribution. They obtained good agreement with direct far-field measurements over the mainbeam and first few sidelobes.

B. First Probe-Corrected Theories (1961–1975)

All of the experimental work of the early period assumed basically that the probe measured a rectangular component of the electric or magnetic vector in the near field. Some early theoretical work [9]–[11] applied approximate correction factors in order to account for the finite size and near-field distance of the measurement probe. In 1961 Brown and Jull [12] gave a rigorous solution to the probe correction problem in two dimensions using cylindrical wave functions to expand the field of the test antenna but plane waves to characterize the probe. However, it wasn't until Kerns [13] reported his plane-wave analysis in 1963 that the first rigorous and complete solution to the probe correction problem in three dimensions became available. Kerns's National Bureau of Standards (NBS) monograph [14], which provides a comprehensive treatment of the "Plane-wave scattering-matrix theory of antennas and antenna–antenna interactions," is the definitive work on the theory of planar near-field scanning. In fact, rigorous three-dimensional probe correction, as pioneered by Kerns, distinguishes modern near-field antenna measurements from less accurate, nonprobe-corrected near-field measurements that could have been formulated shortly after Maxwell published his "Treatise on Electricity and Magnetism."

Probe-compensated cylindrical near-field scanning was extended to three dimensions in 1973 by Leach and Paris [15] of the Georgia Institute of Technology (GIT). Characterizing the probe as well as the test antenna by cylindrical wave functions, they developed the theory, presented sampling criteria, and performed measurements on a slotted waveguide array to verify their technique. Later, Borgiotti [16], using a plane-wave representation for the probe (as in the original paper of Brown and Jull [12]), and Yaghjian [17], using a uniform asymptotic expansion of the Hankel function, derived an approximate probe correction directly from the far field of the probe for cylindrical scanning that approaches the simplicity of the planar probe correction.

The probe-corrected transmission formula for near-field

Manuscript received March 7, 1985; revised October 14, 1985.

The author is with the Electromagnetic Sciences Division, Rome Air Development Center, Hanscom AFB, MA 01731.

IEEE Log Number 8406140.

TABLE I
REPRESENTATIVE ANTENNAS MEASURED AT NBS (FROM [37])

ANTENNA TYPE	FREQUENCY (GHz)	MAJOR DIMENSION IN WAVELENGTHS	GAIN (dB)
HORN LENS	48.0	90	47.0
CONICAL HORN	8.0	6	22.08
CASSEGRAIN REFLECTOR	60.0	91	46.5
CONSTRAINED LENS ARRAY	9.2	23	34.0
PHASED ARRAYS	8.4	17	21.5
	7.5	15	30.5
DIPOLE ARRAY	1.4	5	20.3
FAN-BEAM RADAR	9.5	58	30.0
Ku-BAND REFLECTOR	14.5	60	42.0
Ku-BAND ARRAY	17.00	50	40.0
SHAPED-BEAM REFLECTOR	4.0	20	27.5
MICROSTRIP ARRAY	1.5	27	30.0
PARABOLIC REFLECTOR	1.5-18	15-183	26-47
COMPACT RANGE REFLECTOR	18 & 55	285 & 870	~60.0

scanning in spherical coordinates was derived by Jensen [18] of the Technical University of Denmark (TUD) in 1970. However, the transmission formula could not be "deconvolved" in practice to obtain the required spherical mode coefficients of the test antenna until Wacker's publications [20], [21] of 1974–1975 and Jensen's publication [19] of 1975. These publications showed that the use of a symmetric measurement probe allowed deconvolution through orthogonality of the spherical rotation functions with respect to (ϕ, θ). Wacker [20], [21] also proposed the use of a fast Fourier transform scheme [22] to compute the problematic θ integrals. This scheme was implemented and made more efficient by Lewis [23] and Larsen [24], [25]. An excellent account of probe-corrected spherical near-field antenna measurements at TUD may be found in Larsen's thesis [25].

Wood [26] has developed an alternative spherical scanning technique using a Huygens probe that samples an assumed locally plane-wave field. Recently, Yaghjian and Wittmann [27]–[29] have derived a simplified probe-corrected spherical transmission formula in terms of conventional vector spherical waves. This alternative transmission formula, which is free of rotational and translational addition functions, can be deconvolved by means of the familiar orthogonality of the vector spherical waves. Yaghjian [27] also suggests a direct computation scheme for evaluating the θ integrations.

C. Theory Put into Practice (1965–1975)

The first probe-corrected near-field measurements were conducted at the National Bureau of Standards [30] in 1965 using a lathe bed to scan on a plane in front of a 96 wavelength pyramidal horn radiating at a frequency of 47.7 GHz. For more than 10 years following, probe-corrected near-field scanning was confined to planar and cylindrical scanning at NBS [31]–[35] and GIT, [36], [15], [8] where near-field measurements began around 1968. During that period planar near-field scanning matured at these two laboratories to a fairly routine measurement procedure for directive antennas operating at frequencies from less than 1 GHz to over 60 GHz. Sampling theorems were applied to determine data point spacing, efficient methods of computation were employed, automatic computer-controlled transport of the test antenna and probe was installed, lasers were used to accurately measure the position of the probe, and upper-bound theoretical as well as experimental and computer-simulated error analyses were performed. Table I lists some representative antennas that have been measured at NBS [37].

D. Technology Transfer (1975–1985)

The development of near-field measurements seems to have anticipated the advent of specially designed antennas not well suited to measurement on conventional far-field ranges. During the first ten years of development, near-field antenna measurements were confined to the laboratories of NBS and GIT. The last ten years have seen a much wider interest that includes private industry, as the appeal, but more often the necessity of near-field techniques for measuring certain antennas has stimulated the construction of 50 or more near-field scanning facilities throughout the world. Fig. 1 lists a few of these near-field facilities and their completion dates (second generation dates for NBS and GIT) along with a chart of their

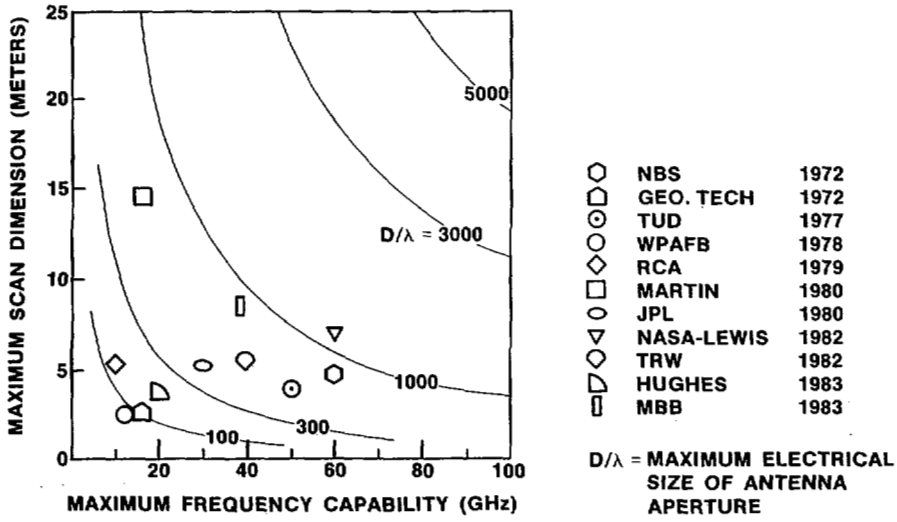

Fig. 1. Some existing near-field facilities (from [38]).

maximum dimensions and frequency capabilities [38]. All the facilities listed in Fig. 1 use the planar, cylindrical, or spherical scanning methods described above, except the Jet Propulsion Laboratory (JPL), which takes planar near-field data on a polar grid rather than on the usual rectangular grid. Like cylindrical scanning, plane-polar scanning requires the probe to move only on a single linear track [39]–[43].

It would be naive to think that the interest in and proliferation of near-field measurement facilities has stemmed solely from an objective evaluation of the scientific merits of near-field techniques. The theory, measurements, and computer programming required to accurately characterize antennas by near-field scanning is considerably more extensive than for conventional far-field measurements. Thus there has been a natural tendency to avoid near-field techniques, often in spite of their advantages, whenever more familiar far-field techniques could be applied.

The recent interest in near-field measurements has been generated primarily by the development of modern, specially designed antennas that are not easily measured on conventional far-field ranges. These antennas include electrically large antennas with Rayleigh distances too large for existing or available far-field ranges; physically large antennas which are difficult to rotate on conventional antenna mounts; array antennas with many elements that can be conveniently interrogated by near-field scanning; reflector antennas with panels that can be accurately aligned by measuring near-field phase; millimeter wave antennas that may experience high atmospheric noise and absorption, especially in inclement weather; antennas with complex far-field patterns for which extensive far-field amplitude (and possibly phase) data are required; antennas with improved and specified polarization properties; delicate antennas that experience high stress and strain under certain rotations or changes in temperature and humidity, and that may require counter balancing and measurement in a controlled environment; nonreciprocal antennas that must be measured in the transmitting mode and thus may be inconvenient for measurement on conventional far-field ranges; classified antennas that must be measured in a secure environment; antennas for which on-site production or field testing is desirable; HF aircraft antennas (3–30 MHz) whose image fields interfere with their free-space patterns being measured directly in the far field (cylindrical scanning has been applied to such HF antennas by D. E. Warren of RADC, Griffiss AFB); and finally antennas with sidelobes too low to be accurately measured on conventional far-field ranges.

The demand on far-field ranges to measure near-in sidelobes that are below -30 dB are severe. For example, as Hansen [44] points out, a far-field distance of at least $6D^2/\lambda$ is required to measure a -49 dB first sidelobe in a Taylor pattern to within 1 dB accuracy. The possibility of determining accurately the patterns of ultralow sidelobe antennas from planar near-field measurements with a probe that has a null in its forward direction (thereby filtering the main beam of the test antenna) has been proposed by Grimm [45], [46] and verified by Newell *et al.* [47]. (Grimm credits Huddleston's thesis [48] for the fundamental ideas suggesting the use of "null probes" for ultralow sidelobe measurements.)

Near-field measurements have also been used in a sophisticated procedure for aligning the beamformers of large, scanning phased array antennas. Specifically, Patton [49] computes the array excitation coefficients by taking the Fourier transform of the complex array factor (far field divided by the element pattern), the far field of which is computed from planar near-field measurements. The entire fundamental period of the array factor is obtained by steering the array to two or more positions, and recording the near-field data for each position. The element pattern can also be evaluated from the planar near-field measurements by steering the array during its measurement and computing the peak values of the steered far-field patterns.

II. Near-Field Theory

A reasonable understanding of the theory of near-field measurements is a prerequisite to a successful near-field

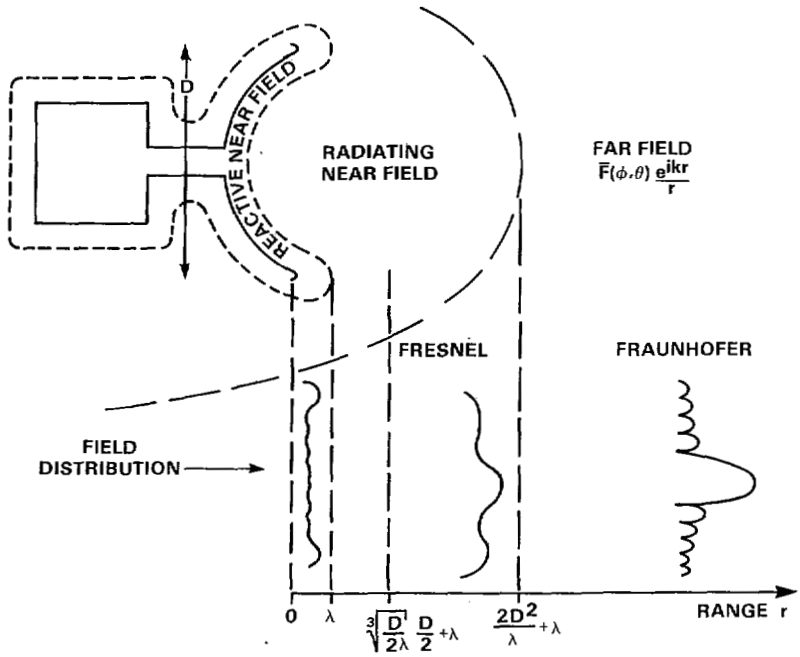

Fig. 2. Exterior fields of radiating antenna.

antenna measurements program. Although not everyone involved in near-field antenna measurements needs to be proficient in the theory, there should be at least one member of the team who gains a competent and versatile knowledge of the theoretical formulation on which the near-field measurements are based.

The references above form a substantial bibliography from which planar, cylindrical, or spherical near-field theory can be studied. A few additional references may prove helpful. Kerns's "translation" [50] of the plane-wave scattering matrix theory of antennas for the measurement of acoustic transducers comprises a streamlined, pedagogical development of planar near-field scanning and extrapolation [51] techniques. The short papers by Kerns *et al.* in *Electronics Letters* [52]–[54], [31] should also be consulted for a brief description of planar near-field analysis. The review paper [55] from GIT applies the Lorentz reciprocity theorem rather than a scattering-matrix approach to derive the probe-compensated planar transmission formula. Appel-Hansen [56] has recently given a useful review of the theory of probe-corrected planar, cylindrical, and spherical near-field measurements. He provides a unified vector wave notation and adopts the source scattering-matrix approach of Yaghjian [17].

Yaghjian [57] can also be referenced for methods to efficiently compute the mutual near-field coupling of two antennas arbitrarily oriented and separated in free space. Given the complex far fields of the two antennas, [57] develops the theory and describes two computer programs for calculating their mutual coupling (or fields) on transverse and radial axes, respectively, in a computer time proportional to the square of the electrical size of the antennas. This rapid evaluation of antenna coupling along radial axes spanning the entire Fresnel region results from the mutual coupling function satisfying the homogeneous scalar wave equation [57].

A. Exterior Fields of Radiating Antennas

Fig. 2 depicts the regions into which the exterior fields of a radiating antenna are commonly divided. The antenna radiates into free space as a linear system with the single-frequency time dependence of exp $(-i\omega t)$. The antenna is assumed ordinary in the sense of not being an extraordinarily highly reactive radiator such as a highly supergain antenna. Another example of a "super-reactive" antenna would be one formed by a number of multipoles located at a single point in space.

The *far-field region* extends to infinity, and is that region of space where the radial dependence of electric and magnetic fields varies approximately as exp $(ikr)/r$. The inner radius of the far field can be estimated from the general free-space integral for the vector potential and is usually set at $2D^2/\lambda + \lambda$ for nonsuper-reactive antennas. (The added λ covers the possibility of the maximum dimension D of the antenna being smaller than a wavelength. In other words, the Rayleigh distance should actually be measured from the outer boundary of the reactive near field of the antenna.) For the main beam direction the Rayleigh distance can sometimes be reduced. However, in the directions of nulls or low sidelobes near the main beam the far field may not accurately form until considerably larger distances are reached [44].

The free-space region from the surface of the antenna to the far field is referred to as the *near-field region.* It is divided into two subregions, the reactive and radiating near field. The reactive near-field region is commonly taken to extend about $\lambda/2\pi$ from the surface of the antenna, although experience with near-field measurements indicates that a distance of a wavelength (λ) or so would form a more reasonable outer boundary to the reactive near field.

The reactive near field can be defined in terms of planar, cylindrical, or spherical modes. Unfortunately, the reactive

fields of spherical (or cylindrical) multipoles are not identical to the plane-wave evanescent fields of the multipoles. Thus, a less ambiguous, simpler, and physically appealing method of defining the reactive region of antennas relies directly on Poynting's theorem and the vector potential. One can show that the contribution to the reactive part of the input impedance of an antenna from the fields outside a surface surrounding the antenna is proportional to the imaginary part of the complex Poynting vector integrated over the surface. Thus, wherever the phase of the electric and magnetic field vectors are near quadrature, the Poynting vector will contribute mainly to the reactive part of the input impedance. Taking the curl of the vector potential integral once to get the magnetic field, and twice to get the electric field shows that the phase of the electric and magnetic fields may be (but are not necessarily) near quadrature in regions within a wavelength (λ) or so of the antenna. Consequently the region within a wavelength or so of the physical antenna is referred to as the *reactive near field.*

Beyond a distance of about a wavelength from nonsuper-reactive antennas, the electric and magnetic fields tend to propagate predominantly in phase, but, of course, do not exhibit exp $(ikr)/r$ dependence until the far field is reached. This propagating region between the reactive near field and the far field is called the *radiating near field.*

Finally, the optical terms, "Fresnel region" and "Fraunhofer region," are sometimes used to characterize the fields of antennas. The term *Fraunhofer region* can be used synonymously with the far-field region, or to refer to the focal region of an antenna focused at a finite distance. The *Fresnel region,* which extends from about $(D/2\lambda)^{1/3}D/2 + \lambda$ to the far field, is the region up to the far field in which a quadratic phase approximation can be used in the vector potential integral. The Fresnel region is a subregion of the radiating near-field region.

B. Scanning with Ideal Probes on Arbitrary Surfaces

Assume we had ideal probes that measured the electric and magnetic fields tangential to an arbitrary surface S enclosing the test antenna, as shown in Fig. 3. Then the Kottler–Franz formulas [58] determine the fields outside S in terms of the E- and H-fields tangential to S. In particular, the far electric field is given by a "vector Kirckhoff integral" of the measured equivalent electric and magnetic currents (see Fig. 3). Although the vector Kirckhoff integral for the far field is fairly simple in form, it requires not only calibrated, ideal probes, but also the measurement of both the tangential electric and magnetic fields over the surface S. In addition, the integral generally takes a relatively large computer time (proportional to $(ka)^3$) compared to planar or cylindrical scanning to obtain one cut in the far-field pattern, where "a" is the radius of the sphere circumscribing the test antenna.

One can derive a modified vector Kirchhoff integral for the electric or magnetic field outside S in terms of the measured tangential electric field alone or the measured tangential magnetic field alone. Fig. 4 gives the formal expression for the electric field outside S in terms of the measured electric field tangential to S and the dyadic Green's function $\bar{\bar{G}}$. However, $\bar{\bar{G}}$ is impractical to find unless S supports orthogonal $\bar{M}$ and $\bar{N}$ vector wave functions, in which case $\bar{\bar{G}}$ is given in terms of $\bar{M}$

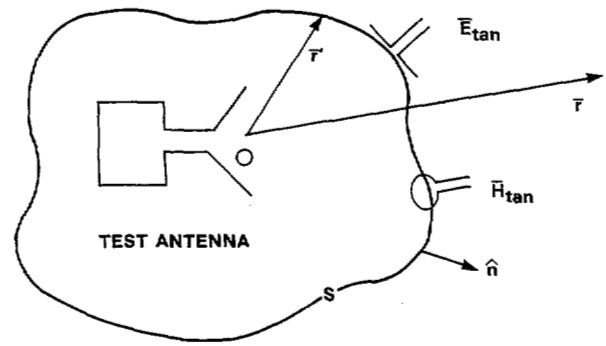

VECTOR KIRCHHOFF INTEGRAL

$$\bar{E}(\bar{r}) = \frac{-ike^{ikr}}{4\pi r}\hat{r} \times \oint_S (\bar{K}_m + Z_o \hat{r} \times \bar{K}_e)\, e^{-ik\hat{r}\cdot\bar{r}'}\, dS' \qquad r \to \infty$$

$$\bar{K}_e = \hat{n} \times \bar{H} \qquad \bar{K}_m = -\hat{n} \times \bar{E}$$

Fig. 3. Scanning with ideal probes on arbitrary surfaces.

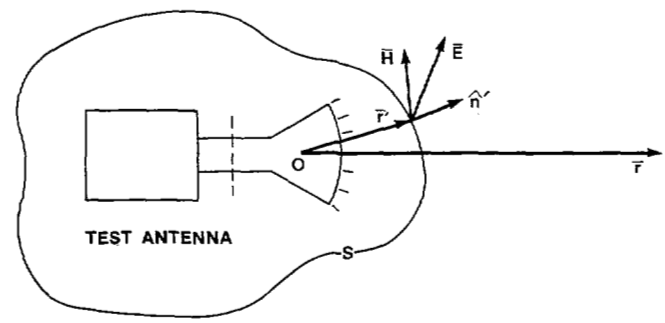

$$\bar{E}(\bar{r}) = \oint_S [\hat{n}' \times \bar{E}(\bar{r}')] \cdot \bar{\bar{G}}(\bar{r}', \bar{r})\, dS'$$

$\bar{\bar{G}}$ IS IMPRACTICAL TO FIND UNLESS S SUPPORTS ORTHOGONAL $\bar{M}$ AND $\bar{N}$ EIGENFUNCTIONS: THEN

$$\bar{\bar{G}}(\bar{r}', \bar{r}) = \sum{}' [\bar{N}^*_m(\bar{r}')\, \bar{M}_m(\bar{r}) - \bar{M}^*_m(\bar{r}')\, \bar{N}_m(\bar{r})]$$

Fig. 4. Fields in terms of $\bar{E}_{tan}$ (or $\bar{H}_{tan}$) only.

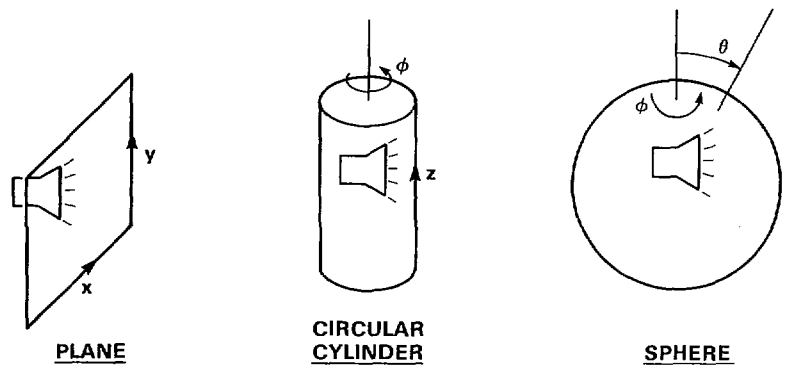

$$\bar{E}(\bar{r}) = \Sigma' T_m^E \bar{M}_m(\bar{r}) + T_m^M \bar{N}_m(\bar{r})$$

ORTHOGONALITY OF $\bar{M}$ AND $\bar{N}$ YIELDS:

$$T_m^E = -\oint_S [\bar{N}_m^*(\bar{r}) \times \bar{E}(\bar{r})] \cdot \hat{n}\, dS; \quad T_m^M = \oint_S [\bar{M}_m^*(\bar{r}) \times \bar{E}(\bar{r})] \cdot \hat{n}\, dS$$

Fig. 5. Scanning with ideal dipole on plane, cylinder, and sphere. (The symbol Σ' denotes integration as well as summation.)

and $\bar{N}$ by the expression at the bottom of Fig. 4. (Note that the $\bar{\bar{G}}$ at the bottom of Fig. 4 is neither the Dirichlet nor the Neumann dyadic Green's function.) There are six coordinate systems that support $\bar{M}$ and $\bar{N}$ vector wave solutions [59], but just three of these—the planar, cylindrical, and spherical—offer mechanically convenient scanning surfaces with simple orthogonal functions. The three other coordinate systems would require scanning on an elliptic cylinder, on a parabolic cylinder, or on a sphere in conical surface coordinates.

C. Scanning with Ideal Probes on Planar, Cylindrical, and Spherical Surfaces

The planar, cylindrical, and spherical scanning surfaces are pictured in Fig. 5 along with the electric field represented by the complete set of $\bar{M}$ and $\bar{N}$ eigenfunctions. After the amplitude and phase of the tangential electric field is measured over the scanning surface S, one finds the unknown transmitting modal coefficients (T_m^E, T_m^M) of the antenna under test by means of the orthogonality integration given in Fig. 5. For simplicity, assume the linear test antenna operates in a single mode of excitation, and that the input coefficient of this feed mode has unity amplitude.

The specific eigenfunction expansions for planar, cylindrical, and spherical scanning, along with their inverse orthogonality integrations for the transmission coefficients are given in Fig. 6. Again note that for each coordinate system, the desired transmission coefficients are determined by a straight-forward double integration of the measured tangential electric field over the scan surface. Similar expressions hold in terms of the tangential magnetic field or in terms of any two independent components of the fields; e.g. James and Longdon [60] formulate spherical scanning in terms of the radial near-field components of the electric and magnetic fields. Explicit expressions for these cylindrical and spherical functions of Fig. 6 in terms of Hankel functions and associated Legendre polynomials, respectively, can be deduced by comparison with similar expressions in [17] and [29]. (The ϕ-integration of the ϕ-component of $\bar{E}_t$ in Fig. 6, and $\bar{b}_t$ in Fig. 8, for cylindrical scanning is done with the unit vector $\hat{\phi}$ held fixed.)

The ideal-probe planar formulas in Fig. 6 as well as the probe-corrected planar formulas in Fig. 8 apply to scanning in rectangular coordinates. Transmission formulas for plane-polar scanning may be found in [39]–[43].

D. Probe Correction for Planar, Cylindrical, and Spherical Scanning

The nonprobe-corrected transmission formulas and their inversions shown in Fig. 6 merely involve the familiar planar, cylindrical, and spherical wave functions of traditional electromagnetic theory [61]. Unfortunately, ideal probes that measure the electric or magnetic field at a point in the near field do not exist in practice. For example, open-ended rectangular waveguide probes commonly used in near-field measurements are less than a wavelength across and yet have far fields that differ appreciably (in the front as well as back hemisphere) from the far fields of elementary magnetic or electric dipoles [62]. Thus, for the accurate determination of electric and magnetic fields from measurements in the near field one must usually correct for the nonideal receiving response of the probe. For planar scanning, probe correction is generally necessary to obtain accurate values of the far field of the test antenna outside the main beam region, regardless of how far the probe is separated from the test antenna. With planar scanning the probe remains oriented in the same direction (usually parallel to the boresight direction of the test antenna), and thus samples the sidelobe field at an angle off the boresight direction of the probe. Planar probe correction simply

PLANAR

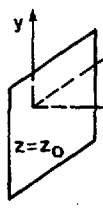

$$\bar{E}_t(x,y,z) = \frac{1}{2\pi}\int_{-\infty}^{\infty}\int_{-\infty}^{\infty} \bar{T}_t(k_x,k_y)e^{i\gamma z}e^{ik_x x}e^{ik_y y}\,dk_x dk_y$$

$$\bar{T}_t(k_x,k_y) = \frac{e^{-i\gamma z_o}}{2\pi}\int_{-\infty}^{\infty}\int_{-\infty}^{\infty} \bar{E}_t(x,y,z_o)e^{-ik_x x}e^{-ik_y y}\,dx dy$$

CYLINDRICAL

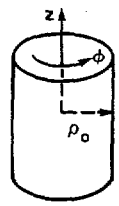

$$\bar{E}_t(\rho,\phi,z) = \frac{1}{2\pi}\sum_{m=-\infty}^{\infty}\int_{-\infty}^{\infty}\left\{\bar{\bar{H}}_m(\gamma,\rho)\cdot\bar{T}_m(\gamma)\right\}e^{im\phi}e^{i\gamma z}\,d\gamma$$

$$\bar{T}_m(\gamma) = \frac{1}{2\pi}\bar{\bar{H}}_m^{-1}(\gamma,\rho_o)\cdot\int_{-\infty}^{\infty}\int_{0}^{2\pi}\bar{E}_t(\rho_o,\phi,z)e^{-im\phi}e^{-i\gamma z}\,d\phi dz$$

SPHERICAL

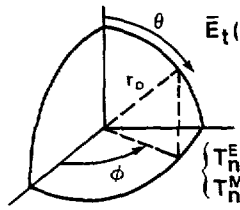

$$\bar{E}_t(r,\phi,\theta) = \sum_{n=1}^{\infty}\sum_{m=-n}^{n}\left[T_{nm}^{E}h_n^{(1)}(kr)\bar{M}_{nm}(\theta) + T_{nm}^{M}g_n^{(1)}(kr)\bar{N}_{nm}(\theta)\right]e^{im\phi}$$

$$\begin{Bmatrix} T_{nm}^{E} \\ T_{nm}^{M} \end{Bmatrix} = \begin{Bmatrix} -h_n^{(1)}(kr_o)^{-1} & \\ & g_n^{(1)}(kr_o)^{-1} \end{Bmatrix}\int_0^{\pi}\int_0^{2\pi}\begin{Bmatrix} \bar{N}_{nm}(\theta) \\ \bar{M}_{nm}(\theta) \end{Bmatrix}\cdot\hat{r}\times\bar{E}(r_o,\phi,\theta)e^{-im\phi}\sin\theta\;d\phi d\theta$$

Fig. 6. Specific expressions for scanning with ideal dipole on plane, cylinder, and sphere.

compensates for this off-boresight sampling by the nonideal probe of the plane waves radiated by the test antenna. For cylindrical scanning, the same argument can be applied in the axial scanning direction to explain why probe correction is generally necessary for cylindrical near-field measurements, regardless of the separation distance between the test and probe antennas.

For spherical scanning, the probe always points toward the test antenna, and thus probe correction becomes unnecessary if the scan radius becomes large enough. However, for spherical near-field measurements within a few diameters of the test antenna, probe correction is generally required to obtain accurate far-field patterns. Fig. 7 shows the far-field pattern computed from nonprobe-corrected spherical near-field data taken at two scan radii from a 25 wavelength, *X*-band array [63]. Comparison with the solid pattern obtained from probe-corrected planar near-field measurements shows that failure to correct for the effect of the probe on spherical near-field data broadens the main beam and smooths out the sidelobes. The broadening of the far-field main beam is caused by the effective narrowing of the near-field beam as the nonideal probe receives from further off its boresight direction the further it gets from the center of the near-field beam. A similar broadening of the far-field pattern from effective near-field narrowing occurs in the azimuthal patterns computed from uncorrected cylindrical near-field data as well [64].

The probe-corrected transmission formulas for planar, cylindrical, and spherical scanning can be found in the relevant references given herein. The probe-corrected transmission formulas for all three scanning geometries are summarized in [56]. Recently, a way has been found to express the probe-corrected transmission formulas for planar, cylindrical, and spherical scanning as a simple modification of the nonprobe-corrected formulas [65], [27]–[29]. By defining the vector output of a probe as its response in the two orthogonal orientations required for complete planar, cylindrical, or spherical near-field measurements, the probe-corrected formulas become similar in form to the uncorrected formulas of Fig. 6. Specifically, these vector probe-corrected formulas shown in Fig. 8 can be obtained from the ideal-probe formulas of Fig. 6 by first replacing the measured tangential *E*-field with $\bar{b}_t$, the vector response of the arbitrary probe, then vector multiplying the unknown transmission coefficients of the test antenna by the receiving coefficients of the probe. Once the

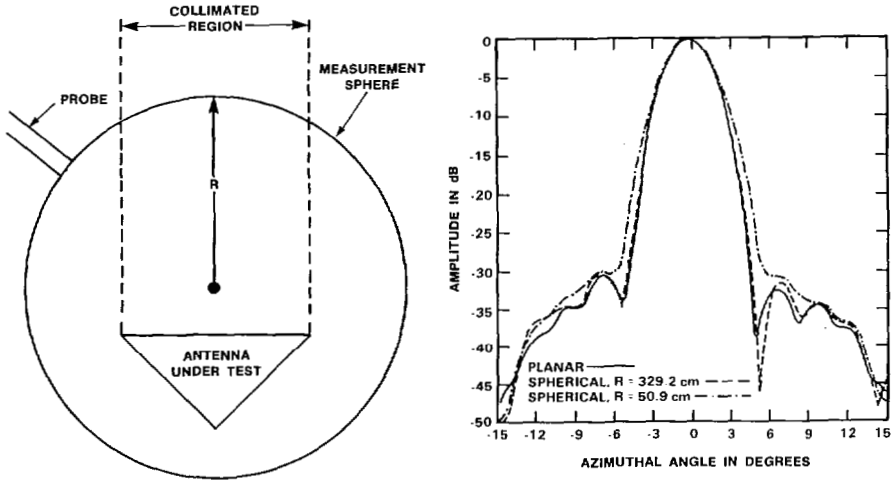

Fig. 7. Effect of probe correction for spherical scanning (from [63]).

PLANAR

$$\bar{b}_t(x,y,z) = \frac{1}{2\pi}\int_{-\infty}^{\infty}\int_{-\infty}^{\infty} \bar{\bar{R}}(k_x,k_y)\cdot \bar{T}_t(k_x,k_y)\, e^{i\gamma z} e^{ik_x x} e^{ik_y y}\, dk_x dk_y$$

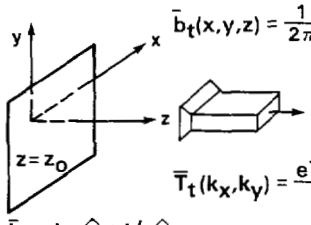

$$\bar{T}_t(k_x,k_y) = \frac{e^{-i\gamma z_o}}{2\pi}\bar{\bar{R}}^{-1}\cdot\int_{-\infty}^{\infty}\int_{-\infty}^{\infty} \bar{b}_t(x,y,z_o) e^{-ik_x x} e^{-ik_y y}\, dx dy$$

$$\bar{b}_t \equiv b_p \hat{x} + b'_p \hat{y}$$

CYLINDRICAL

$$\bar{b}_t(\rho,\phi,z) = \frac{1}{2\pi}\sum_{m=-\infty}^{\infty}\int_{-\infty}^{\infty}\left\{\bar{\bar{R}}_m(\gamma,\rho)\cdot\bar{T}_m(\gamma)\right\} e^{im\phi} e^{i\gamma z}\, d\gamma$$

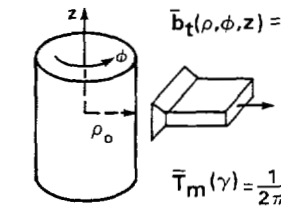

$$\bar{T}_m(\gamma) = \frac{1}{2\pi}\bar{\bar{R}}_m^{-1}(\gamma,\rho_o)\cdot\int_{-\infty}^{\infty}\int_{0}^{2\pi} \bar{b}_t(\rho_o,\phi,z) e^{-im\phi} e^{-i\gamma z}\, d\phi dz$$

$$\bar{b}_t \equiv b_p \hat{\phi} + b'_p \hat{z}$$

SPHERICAL

$$\bar{b}_t(r,\phi,\theta) = \sum_{n=1}^{\infty}\sum_{m=-n}^{n}\left[T^E_{nm} R^E_n(r)\bar{M}_{nm}(\theta) + T^M_{nm} R^M_n(r)\bar{N}_{nm}(\theta)\right] e^{im\phi}$$

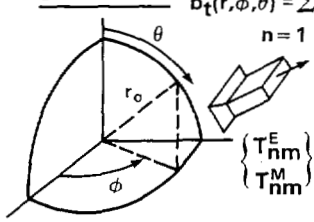

$$\begin{Bmatrix} T^E_{nm} \\ T^M_{nm} \end{Bmatrix} = \begin{Bmatrix} -R^E_n(r_o)^{-1} \\ R^M_n(r_o)^{-1} \end{Bmatrix}\int_0^{\pi}\int_0^{2\pi}\begin{Bmatrix} \bar{N}_{nm}(\theta) \\ \bar{M}_{nm}(\theta) \end{Bmatrix}\cdot \hat{r}\times\bar{b}_t(r_o,\phi,\theta)\, e^{-im\phi} \sin\theta\, d\phi d\theta$$

$$\bar{b}_t \equiv b_p \hat{\phi} + b'_p \hat{\theta}$$

Fig. 8. Probe-corrected formulas. (The vector response of the probe is denoted by $\bar{b}_t$.)

PLANAR

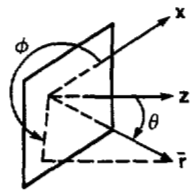

$$\bar{E}(r,\phi,\theta) = \frac{-ike^{ikr}}{r} \cos\theta\, \bar{T}(k\sin\theta\cos\phi,\ k\sin\theta\sin\phi)$$

CYLINDRICAL

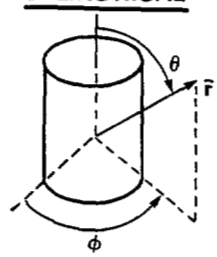

$$\bar{E}(r,\phi,\theta) = \frac{-2ke^{ikr}}{r} \sin\theta \sum_{m=-\infty}^{\infty} (-i)^m \left[\bar{T}_m(k\cos\theta)\right] e^{im\phi}$$

SPHERICAL

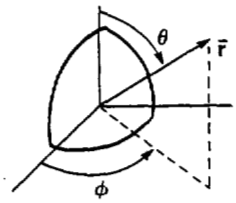

$$\bar{E}(r,\phi,\theta) = \frac{-ie^{ikr}}{r} \sum_{n=1}^{\infty} \sum_{m=-n}^{n} (-i)^n \left[T^E_{nm}\bar{M}_{nm}(\theta) + T^M_{nm}\bar{N}_{nm}(\theta)\right] e^{im\phi}$$

Fig. 9. Far electric field.

receiving coefficients of the probe are obtained from the far fields of the probe, the probe-corrected near-field formulas reduce to the simplicity and familiarity of the uncorrected electric or magnetic field formulas in planar, cylindrical, and spherical coordinate systems. (The mismatch factor involving the reflection coefficients of the probe and its termination are absorbed into the receiving coefficients of Fig. 8.)

The only restrictive assumption in the theory leading to the probe-corrected formulas of Fig. 8 is that multiple reflections between the probe and test antennas are negligible. For the spherical scanning formulas of Fig. 8, the receiving pattern of the probe is assumed to have first-order azimuthal dependence only.

E. Expressions for the Far Field

After the transmission coefficients of the test antenna are computed from the double orthogonality integrals of the measured data (and probe correction is applied, if necessary), the amplitude and phase of the electric field outside the test antenna can be computed from its modal expansions given in Fig. 6. Usually, the far fields of the test antenna are of primary concern. They are obtained through asymptotic evaluation of the modal expansions, and are shown explicitly in Fig. 9 for each of the three scanning geometries. The far fields are determined from the transmission coefficients of the test antenna directly for planar scanning, by a single summation for cylindrical scanning, and by a double summation for spherical scanning. And, of course, the far-field patterns (co-polar and cross-polar), polarization (axial ratio, tilt angle, and sense), directivity and gain of the test antenna derive directly from the electric or magnetic far field. Integration of the difference between the gain and directivity functions obtained from near-field measurements determines the "ohmic" losses of antennas.

The receiving characteristics of reciprocal antennas can be determined from the radiating characteristics through the reciprocity relations. For nonreciprocal antennas the receiving properties can be obtained from near-field measurements by transmitting with the probe antenna, or, if possible, by converting the test antenna to its adjoint antenna [14], [17], [25], [66].

III. Sampling Theorems and Efficient Methods of Computation

Richmond and Tice, [4], [5] in the earliest papers (of which I am aware) that computed the far-field pattern from near-field measurements (nonprobe-corrected), assumed separable near fields because as Richmond [5] states, "while the solution may be simple in principle, in practice the numerical computation is tedious and may require the use of large computers." Kyle

[6] also mentioned that computing the far field from the near-field data of electrically large antennas would be "difficult" on the computers available in 1958. These early statements of Richmond and Kyle emphasize the important role that high speed computers, fast Fourier transforms, and rigorous sampling theorems have played in the development of near-field techniques.

A. Sampling Theorems

Before the far fields can be determined from the expressions in Figure 9, the transmission coefficients must be evaluated from the double integrals in Fig. 8 (or Fig. 6 for no probe correction) of the measured near-field data. Probably the simplest way to evaluate the integrals is to replace them by summations over constant increments in $\Delta x \Delta y$, $\Delta\phi\Delta z$, and $\Delta\phi\Delta\theta$ for planar, cylindrical, and spherical measurements. Ordinarily this use of the elementary rectangular rule of integration would be an approximation that introduced computational errors unless the sample increments approached zero. Fortunately, the transmission coefficients can be shown to be bandlimited, and thus modern sampling theorems [67] can be applied to prove that the conversion of the integrals to summations introduces no error (or negligible error since real antennas are not quite perfectly bandlimited) if the sample increments are chosen less than a given finite value. Specifically, for planar scanning the $\bar{T}(k_x, k_y)e^{i\gamma z_0}$ becomes negligible beyond $k_x^2 + k_y^2 = k^2$ (for separation distances greater than a few wavelengths) and thus the sampling theorem yields the maximum data point spacing of $\Delta x = \Delta y = \lambda/2$. For cylindrical scanning the $\bar{T}_m(\gamma)$ are bandlimited by $\pm k$ in γ and $\pm k(a+\lambda)$ in m to allow the sample spacings of $\Delta z = \lambda/2$ and $\Delta\phi = [\lambda/2(a + \lambda)]$. The brackets indicate the largest number, equal to or smaller than the bracketed number, that divides 2π into an integer number of divisions. For spherical scanning, the T_{nm} are bandlimited by $k(a + \lambda)$ in both m and $\pm n$, to give identical angular sample increments of $\Delta\phi = \Delta\theta = [\lambda/2(a + \lambda)]$. Actually the sampling theorem applies only approximately to the direct θ-integration of spherical scanning because the limits of integration span π rather than 2π [27]. An alternative Fourier transform method [22] has been developed by Wacker [20], [21], Lewis [23], and Larsen [24], [25] that avoids this extra, albeit slight, approximation.

Fig. 10 summarizes the sampling criteria for the three conventional scanning surfaces as well as for plane-polar scanning. A question mark attends the sample spacing of $\lambda/2$ for the radial direction because no rigorous sampling theorem with uniform spacing has been derived for the radial functions of plane-polar scanning. The sampling theorem and Fourier transform have been applied indirectly to the radial integration but only for the nonuniform sample spacing [42] required by the "quasifast Hankel transform" [68]. Also, the linear distance between the plane-polar angular sampling points for $\rho < a$ can probably be increased to $\lambda/2$ for most antennas without introducing serious aliasing errors.

One of the attractive features of spherical scanning is that the angular sampling increments remain the same for all scan radii. Thus, as one scans further from the antenna the linear distance between data points becomes larger to keep the total

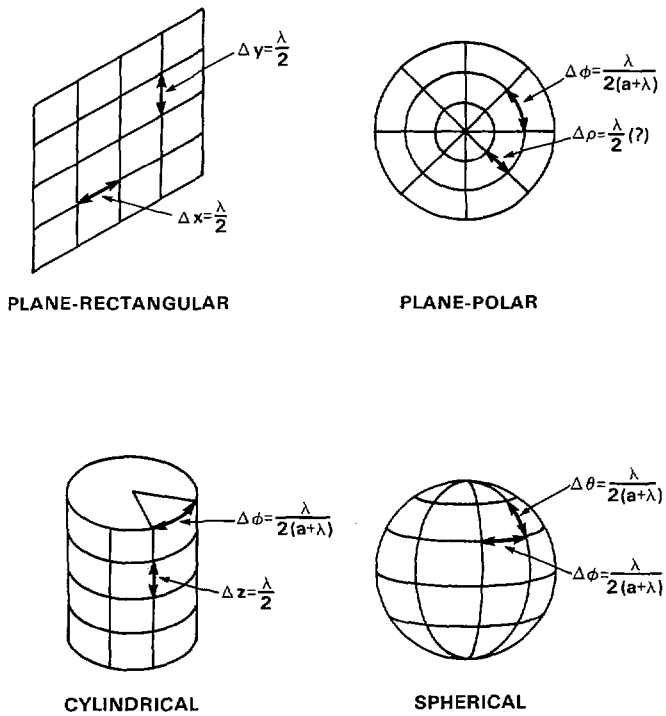

Fig. 10. Sampling spacing. ("a" is the circumscribing radius of the antenna measured from the center of rotation.)

required sample points for each polarization at a fixed number of about $2(ka + 2\pi)^2$. Similarly, the angular sampling increments of cylindrical and plane-polar scanning are independent of the scan radius. However, for the axial sampling of cylindrical scanning, the radial sampling of plane-polar scanning, and the xy rectangular sampling, the data point spacing must approach $\lambda/2$, as the scan distance approaches infinity, regardless of how large a separation distance is chosen between the probe and test antenna, in order to sample the rapid phase variation the probe encounters in the far-out sidelobe region. Of course, if the far field is required only near the main beam direction, the sampling increments for all of the scan techniques can usually be increased without introducing serious aliasing errors.

The sampling criteria shown in Fig. 10 assumes that the separation distance between the probe and test antennas is large enough to prevent significant coupling of their reactive fields. For nonsuper-reactive antennas, a few wavelengths of separation is usually sufficient. However, if the probe scans within the reactive fields of the test antenna, the sampling increments must be decreased to assure accurately computed far fields. The decreased sample spacing (Δs) required for planar, cylindrical, or spherical near-field measurements at a separation distance (d) of a few wavelengths or less between nonsuper-reactive probe and test antennas can be estimated from the simple formula,

$$\Delta s = \frac{\lambda}{2\sqrt{1+\left(\frac{\lambda}{d}\right)^2}},$$

which can be obtained by setting $\alpha_{\min}$ to 54.6 dB in Joy and

Paris [36, eq. (11)]. For example, at a separation distance of about half a wavelength, the distance between data points should generally be less than $\lambda/4$ to compute accurate far fields (assuming negligible multiple reflections which, if present, can decrease appreciably the required sample spacing Δs).

The reactive fields of the test antenna inside the scan surface on which the near-field data was taken cannot, in general, be computed with high accuracy because the probe will not have been sufficiently excited by the rapidly decaying reactive fields that can dominate close to the test antenna. Although useful rough approximations to the fields inside the reactive zone can often be computed from the limited spectrum used to represent the fields outside the reactive zone [69].

B. Efficient Methods of Computation

Sampling theorems have converted the deconvolution integrals (shown in Fig. 8 or 6) for the transmission coefficients to double summations and have provided convenient criteria for the data-point spacing. (In practice, the infinite limits of integration in the planar and cylindrical cases are replaced by the finite limits of the scan surface.) For large antennas the plane-rectangular summations take a computer time proportional to $(ka)^2$ for one cut (one k_x or k_y) in the far field whether or not the fast Fourier transform (FFT) is used. With the FFT the entire planar far field can be computed in a time proportional to $(ka)^2 \log_2 ka$. Similarly, the cylindrical summations take a computer time proportional to $(ka)^2$ for one azimuthal cut in the far field, and proportional to $(ka)^2 \log_2 ka$ for the entire far field using the FFT.[1]

As Fig. 9 shows, with spherical scanning all the transmission coefficients are required, in general, for just one cut in the far field. In addition, the double summations in Fig. 9 and in Fig. 8 for the transmission coefficients take a computer time proportional to $(ka)^3$ whether summed directly [27] or using the FFT [20], [21], [23]–[25]. Similarly, the plane-polar computation of the transmission coefficients takes a computer time proportional to $(ka)^3$ for direct evaluation of either the Fourier integral or orthogonal-function coefficients [39]–[42], and proportional to $(ka)^2 \log_2 ka$ using the "quasifast Hankel transform" (FHT) [42], [68] for one or more far-field cuts. However, the FHT requires nonuniform data spacing in the radial direction, it still takes 20–30 times longer than the FFT applied to uniform xy sampling, and it has not yet been utilized for near-field measurements [42].

The computation times on a Cyber 750 for planar, cylindrical, and spherical scanning are displayed in Fig. 11. All the computer times remain quite manageable even for electrically large antennas, except for spherical scanning and plane-polar scanning. Computer times for these two techniques quickly grow into the hours for antennas larger than 100 wavelengths in diameter. And, of course, on many minicomputers, the

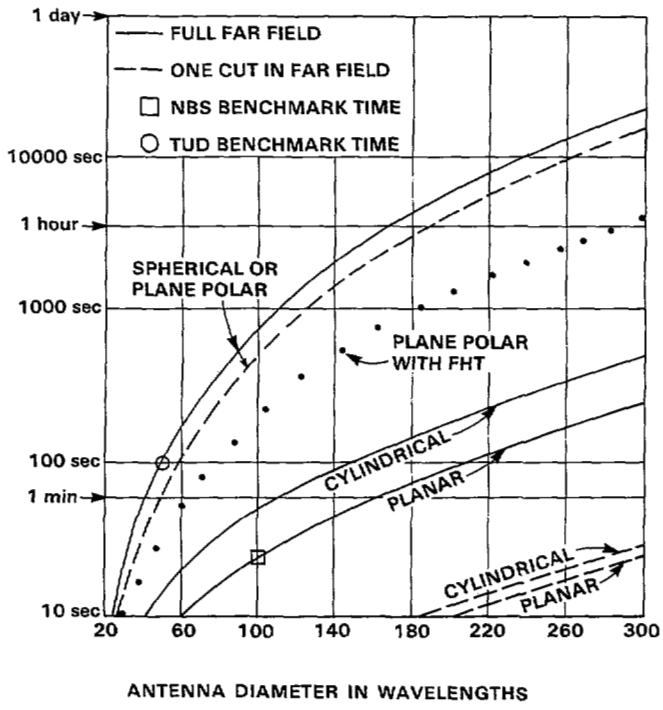

Fig. 11. CPU time for NF to FF transformation on Cyber 750.

computations for any of the techniques would take considerably longer than on the Cyber 750. However, if only the main beam and near-in sidelobes of the antenna are required, or if the near fields of the antenna display a suitable symmetry, sampling increments can usually be increased, and computer times may decrease substantially.

In applying the FFT to conventional plane-rectangular measurements, one must consider the resolution one wants in the far-field pattern. A straightforward application of the FFT to near-field data taken at the usual $\lambda/2$ data point spacing specified by the sampling theorem generates output at points too widely spaced to smoothly resolve the far-field pattern. For single cuts in the far-field only a one-dimensional FFT is required, and one can increase the resolution (i.e., decrease the angular separation between far-field points) merely by "zero-filling" the near-field data. Unfortunately, sufficient zero-filling of a two-dimensional FFT that generates the entire far field of an electrically large antenna may require more on-line central memory than some computers provide. To obtain the complete highly resolved pattern with such computers, one can resort to computing the discrete double Fourier transform directly in a time proportional to $(ka)^3$, or if this computer time is prohibitive, one can use an off-line version of the two-dimensional FFT. Off-line (mass-storage) versions of the FFT are readily available or can be programmed straightforwardly starting with a one-dimensional FFT algorithm [70]. For the Cyber 750 at NBS, mass-storage versions of the FFT take an input/output time typically equal to the central processing time [71]. Of course, a larger core storage or virtual memory capability may eliminate the need for mass-storage versions of the two-dimensional FFT.

[1] We are assuming the computer times using the FFT are minimized by choosing (or padding) the number of near-field data points to equal 2^N, where N is a positive integer.

IV. Experimental Errors

The theory of near-field antenna measurements applies rigorously to linear antennas radiating or receiving in a single mode at a fixed frequency, and satisfying Maxwell's equations in free space. The antennas may be nonreciprocal, lossy, lossless, or "gainy." The only restrictive assumption involved in the theory of probe-corrected near-field measurements is that multiple reflections between the probe and test antennas are negligible. However, in practice experimental errors limit the accuracy of near-field techniques. In addition to the multiple reflections, the experimental measurements will introduce probe positioning errors, instrumentation errors, and for the planar and cylindrical (or truncated spherical) scanning geometries, finite scan errors. Errors are also introduced by room reflections, uncertainties in the far field of the probe, and in the measurement of the insertion loss between the test antenna and probe when absolute gain is required. (If sample spacing and computer accuracy are adequate, aliasing and computational errors will be negligible compared to the experimental errors.)

Upper-bound error analyses [34], [35], as well as computer simulations [35], [72], [73], have been performed for determining the accuracy of the far field obtained from planar near-field measurements. Computer simulations have also been performed for cylindrical [74], [75] and spherical [18], [76] near-field scanning, but an analytical treatment of upper-bound errors for near-field measurements on a cylinder or sphere remains outstanding.

The relative importance of the various near-field measurement errors upon the far field depends, of course, on the antenna under test, the frequency of operation, the measurement facility, and the probe. However, the results of the planar upper-bound error analyses [34], [35] show that for typical microwave antennas and planar near-field testing facilities, three or four sources of error dominate: finite scan area, z-position of the probe, receiver nonlinearities in measuring the near-field amplitude, and sometimes, multiple reflections.

The effects on the far field of limiting the planar measurements to a finite scan area are small for highly directive antennas well within the "solid angle" formed by the edges of the test antenna and the edges of the finite scan area. Outside this solid angle, the far fields cannot be relied upon with any confidence. Although for very highly tapered near fields this solid angle can be extended somewhat [75], since the effective radiating aperture of a highly tapered illumination is somewhat smaller than the physical aperture.

The z-position inaccuracies, i.e., the deviation from planarity of the probe transport over the scan area, can produce relatively large errors in the sidelobe levels of the far field. Variations in the z-position of the probe produce corresponding variations in the near-field phase. Thus, large errors in the sidelobes occur in the far-field directions corresponding to the predominant spacial frequencies of the variation in z-position across the scan area. In the main beam direction, the effect of z-positioning of the probe is much less critical—the reduction in gain being given by $\delta^2/2$, the familiar Ruze relation [77], [34]. The errors in the sidelobes caused by inaccurate z-positioning can be reduced by measuring the deviation of the probe from the scan plane and correcting the near-field phase proportionately [78], [79], [33]. Alternatively, the position of the probe may be corrected mechanically by a servomechanism. It should also be mentioned that receiver phase errors generally have a much smaller effect on the far field than phase errors caused by inaccurate z-positioning, because typical receiver phase errors are negligible at the maximum near-field amplitude and increase monotonically with decreasing amplitude [35].

Receiver nonlinearities in the measurement of near-field amplitude, however, can cause significant errors in the main beam and sidelobes of the far fields. For example, a receiver nonlinearity of ± 0.02 dB/dB can produce several tenths of a dB error in gain, and a several dB error in a 35 dB sidelobe of a typical microwave reflector. Fortunately, these receiver amplitude errors can be greatly reduced by calibrating the receiver, e.g. with a precision attenuator, and applying the calibration curve to the near-field data [33].

The contribution to the output of the probe from the multiple reflections can be estimated by changing the separation distance between the probe and test antenna and recording the amplitude variations that occur in the received signal with a period of about $\lambda/2$. If multiple reflections prove significant, they may be reduced by the judicious use of absorbing material, by decreasing the size of the probe, by increasing the probe separation distance, by averaging the far fields computed from the near-field data taken on scan planes that are separated by a small fraction of a wavelength (say $\lambda/4$ or less), or by using specially designed probes that filter the main beam and accentuate the sidelobes [45]–[47].

Finally, the upper-bound error formulas [34], [35] should be applied with discretion. They are dependent upon underlying (usually explicitly stated) assumptions that are satisfied by most antennas and near-field measurement conditions, but which may be either violated or relaxed in certain circumstances. For example, it is well-known that phase errors introduced into the main near-field beam of directive antennas cause a reduction in the computed on axis gain [77], [34]. However, this gain reduction strictly applies to near-field beams of uniform phase and will not hold for antennas with variations in their phase if the phase errors occur in just the right places and with just the right values to eliminate the original phase variations. Although this conjunction of phase variations is highly unlikely, its possibility of occurrence is revealed from an examination of the error analyses [34], [35].

When the underlying assumptions can be relaxed, lower upper-bounds can usually be obtained. For example, an estimate of the specific z-position errors for a particular measurement facility allows one to estimate their effect upon far-field sidelobes more accurately than with the general upper-bound expressions [35].

V. Limitations of Near-Field Scanning

We conclude this overview pointing out some of the present limitations of measuring antennas by scanning in the near field.

Planar, cylindrical, and spherical near-field scanning can be

formulated to include all the multiple interactions between the probe and test antennas [14], [17], [25]. However, deconvolution to solve for the transmitting or receiving properties of the test antenna can be accomplished, in general, with the existing formulations only when multiple interactions are neglected. The scattering properties of both the probe and test antenna would be required in a general deconvolution scheme that included multiple interactions. It may be possible to estimate the scattering from certain antennas, or to calculate the scattering from canonical antennas such as the perfectly conducting or dielectric sphere [14]. However, the complete scattering characteristics of antennas are not generally available nor is the determination of scattering along with transmitting/receiving properties presently feasible using near-field techniques. Moreover at frequencies below a few hundred megahertz, absorbing materials that reduce multiple interactions and room reflections to acceptable levels may be difficult or expensive to obtain.

Of course, scattering from passive objects can be determined from scanning in the near field simply by viewing the scattered fields as the transmitted fields of a radiating test antenna, and, as usual, neglecting multiple interactions. Recently Dinallo [80] has formulated a planar-scan method of measuring passive scatterers that involves moving an illuminating "probe" in the near field, as well as the measuring probe, in order to synthesize an incident plane wave. The method requires that the usual two-dimensional Fourier transforms of planar near-field deconvolution be applied to the output of the measuring probe for each position of the illuminating probe.

All three near-field scanning techniques—planar, cylindrical, and spherical—require that the output of the probe be measured in amplitude and phase[2] over the scan surface. This requirement obviously restricts near-field techniques to antennas that are limited in physical size and frequency. The test antenna cannot be appreciably larger in linear dimensions than the extent of the probe transport on planar and cylindrical near-field ranges (although the effective scan area can sometimes be increased by shifting the position of the test antenna) nor larger than the model mount will handle on spherical ranges where the probe is fixed and the test antenna rotates through the two spherical angles. (Of course, this latter restriction limits far-field ranges as well.) In addition, since the near-field phase must generally be measured to within a small fraction of a wavelength to obtain accurate far fields, most existing near-field scanners are limited to antennas that operate at frequencies below 40–100 GHz.

Measurement and computation times may make near-field scanning unattractive for antennas that are extremely large electrically. Since amplitude and phase data must usually be recorded at roughly $2(ka)^2$ points in the near field for each polarization at each frequency of operation, it will take many hours to scan an antenna one hundred wavelengths across if the scan rate, for example, is on the order of one data point per second. Long scan times not only limit frequent and repeated experimentation but also demand a more stable measurement system.

Fortunately, the computer time required to process plane-rectangular and cylindrical near-field scan data amounts typically to a few minutes for antennas hundreds of wavelengths across (see Fig. 11), and thus plane-rectangular and cylindrical near-field scanning is presently measurement-time limited rather than computer-time limited. Conversely, spherical near-field scanning and plane-polar scanning with uniform sample spacing in the radial direction requires computing times proportional to $(ka)^3$ (see [24], [25], and [42]), and thus these two techniques are presently computer-time limited because, as mentioned above, measurement time grows as $(ka)^2$.

There is another limitation (besides the neglect of multiple reflections) within the basic theory of planar near-field scanning that limits the application of planar scanning to directive antennas. The output of the probe behaves asymptotically as $\exp(ikr)/r$ as the probe scans on a near-field plane away from the test antenna. Inserting this asymptotic behavior into the two-dimensional Fourier transform of the near-field data shows that the computed plane-wave spectrum for $K = 0$, i.e., the computed on-axis far-field of the test antenna, will retain an oscillating contribution whose amplitude remains finite even as the dimensions of the scan area approach infinity [34], [57]. In other words, the computed far field of the test antenna will be in error by an amount that does not approach zero as the planar scan area approaches infinity. In practice, this planar-scan error can be shown to be negligible for directive antennas [34]. However, for broad-beam antennas it can prevent the accurate determination of the far field using planar near-field scanning [82]. And, of course, planar scanning is limited in general to determining the fields within the forward solid angular region subtended by the edges of the test antenna and the finite scan area [34]. (Spherical scanning gives full pattern coverage and cylindrical scanning omits only the biconical angular region formed by the outer edges of the test antenna and the cylindrical scan area of finite height.)

Although plane-polar scanning, like cylindrical scanning, has the mechanical advantage of requiring the probe to move along a single linear track, it has several disadvantages that do not accompany plane-rectangular scanning. In order to apply probe-correction to plane-polar near-field measurements, the probe must be rotated along with the test antenna [39]–[42]. To avoid this extra complicating mechanical rotation, plane-polar measurements to date have not included probe correction and thus have been limited to using small probes and to computing far fields within a small angle of the forward direction [39], [40]. As mentioned in Section III-A, there exists no rigorous sampling theorem for equal radial increments in plane-polar scanning; thus one cannot be assured that negligible error will be introduced by sampling at $\lambda/2$ increments in the radial direction. Computation times, as shown in Fig. 11, for plane-polar scanning grows as $(ka)^3$ for

[2] In principle, phase can be obtained indirectly from an additional amplitude scan performed after a known reference signal is added to the original signal from the test antenna. This "microwave holographic" technique for determining phase from two amplitude scans has been further simplified to require just one amplitude scan if the phase of the reference signal is shifted linearly with the position of the probe, and the near-field is oversampled [81].

either direct summation of the near-field Fourier integral converted to polar coordinates, or straightforward evaluation of orthogonal-function expansions like the Jacobi–Bessel series [39]–[43]. This implies many hours of computer time on commonly available main frames to obtain the complete patterns of antennas a hundred wavelengths or more in diameter. Computer times on slower minicomputers would increase proportionally. Reduced computer times for plane-polar scanning may be attained with the "fast Hankel transform." However, the FHT method of computation requires unequal sampling increments in the radial direction, and evidently has not been implemented [42]. Plane-polar systems could, in principle, be devised to sample data on a rectangular grid, or data in polar coordinates could be interpolated to obtain data on a rectangular grid, thereby allowing one to compute the far field by means of the fast Fourier transform. The former modification, however, requires an appreciably more sophisticated control system for the near-field scanner, and the latter introduces errors into the near-field data.

Use of the Jacobi–Bessel series [39]–[41] to expand the near-field data of plane-polar scanning has a couple of further limitations that should be recognized. Although the Jacobi–Bessel functions are orthogonal on a plane, they do not form part of a separable solution to Maxwell's equations. Thus, the Jacobi–Bessel coefficients can be used to compute the far field of the test antenna, but unlike the cylindrical, spherical, or plane-rectangular coefficients, they cannot be used to compute directly the fields between the test antenna and the far field [41]. One has to resort to indirect methods to compute efficiently the near fields from the Jacobi–Bessel coefficients, such as converting the polar far field to a plane-wave spectrum in rectangular coordinates and integrating the spectrum in k-space to obtain the near fields. Secondly, the large computer time proportional to $(ka)^3$ required for plane-polar data processing with the Jacobi–Bessel series is not directly reducible using the fast Hankel transform as is the computation time using the orthogonal Hankel transform series that form the naturally separable solutions in plane-polar coordinates [42], [43].

There are also limitations and disadvantages accompanying cylindrical and spherical scanning. Most directive antennas display approximately planar wavefronts over their main near-field beams. Thus one can often learn a great deal about the operation of the test antenna merely by plotting the amplitude and phase of the measured near-field data taken on planes parallel to these wave fronts. For instance, Repjar and Kremer [83] were able to align the panels of a millimeter-wave reflector by plotting the phase contours of near-field data taken on a plane in front of the reflector. Similarly, faulty array elements or banks of elements are often revealed directly in plots of planar near-field data. It is considerably more difficult to take near-field data on planes in front of the test antenna with cylindrical and spherical near-field ranges where the probe is incapable of direct two dimensional scanning in a plane. (Granted, the far field obtained from cylindrical or spherical near-field data could be converted to a plane-wave spectrum and the near fields on planes in front of the test antenna could be computed as the Fourier transform of this plane-wave spectrum.) Secondly, some antennas may be too heavy, too fragile, or too deformable to rotate precisely through two spherical angles or even one cylindrical angle. (For such antennas spherical or cylindrical scanning could still be applied, in principle, by fixing the antenna and moving the probe on a sphere or cylinder surrounding the antenna.) Thirdly, although much progress has been made in simplifying the probe correction for cylindrical [16], [17] and spherical [20], [21], [27]–[29] near-field scanning, it remains more difficult to formulate, understand, and apply than for planar scanning. Fourthly, convenient upper-bound expressions for far-field parameters determined from errors in near-field measurements have not been obtained for cylindrical and spherical scanning as they have been for planar scanning [34], [35]. A great deal of information on far-field accuracy can be obtained from computer simulations applied to hypothetical and measured cylindrical and spherical near-field data [74]–[76]. In addition, some of the results from the planar error analyses can be reinterpreted to estimate the effect of errors in cylindrical and spherical scanning. (For example, the simple solid-angle criterion [34] for the validity of far fields computed from near-field data on truncated planes can be applied to truncated cylinders and spheres as well.) Nevertheless, general, convenient, analytic estimates of accuracy for cylindrical and spherical near-field scanning remain undetermined.

Finally, by ending a paper with a discussion of the limitations of near-field scanning techniques, one risks discouraging the use of near-field scanning as an alternative to more direct antenna measurement methods, which, of course, have their own problems and limitations. Therefore, let us end with a quote from the paper by Kummer and Gillespie [84] who surveyed the major near, intermediate, and far-field methods available in 1978 for measuring antennas, and concluded that "the near-field (scanning) technique may well become accepted as the most accurate technique for the measurement of power gain and of patterns for antennas that can be accommodated by the measuring apparatus." The evidence of the intervening years supports their conclusion.

Acknowledgment

As the main text and references attest, this overview could not have been written without the decade of working in the Antenna Systems Metrology Section of the National Bureau of Standards, Boulder, CO, especially with D. M. Kerns, A. C. Newell, R. C. Baird, P. F. Wacker, C. F. Stubenrauch, R. L. Lewis, R. C. Wittmann, A. G. Repjar, D. P. Kremer, M. L. Crawford, E. B. Miller, and M. H. Francis.

References

[1] R. M. Barrett and M. H. Barnes, "Automatic antenna wavefront plotter," *Electron.*, vol. 25, pp. 120–125, Jan. 1952.

[2] R. E. Collin and F. J. Zucker, *Antenna Theory*, pt. II. New York: McGraw-Hill, 1969, ch. 17.

[3] G. A. Woonton, "On the measurement of diffraction fields," in *Proc. McGill Symp. Microwave Opt.*, (AFCRC-TR-59-118(II)), 1953, pp. 347–350.

[4] J. H. Richmond and T. E. Tice, "Probes for microwave near-field measurements," *IRE Trans. Microwave Theory Tech.*, vol. MTT-3, pp. 32–34, Apr. 1955.

[5] J. H. Richmond, "Simplified calculation of antenna patterns with

application to radome problems," *IRE Trans. Microwave Theory Tech.*, vol. MTT-3, pp. 9–12, July 1955.

[6] R. F. Kyle, "Far-field radiation of a cheese aerial," *Electron. Radio Eng.*, vol. 35, pp. 260–262, July 1958.

[7] L. Clayton, Jr., J. S. Hollis, and H. H. Teegardin, "A wide frequency range microwave phase-amplitude measuring system," in *Abstracts 11th Annu. USAF Symp. Antenna Res. Development,* Univ. Illinois, Oct. 1961 (Also published in the *Essay*, Sci.-Atlanta, no. 4, Sept. 1963.)

[8] R. C. Johnson, H. A. Ecker, and J. S. Hollis, "Determination of far-field antenna patterns from near-field measurements," *Proc. IEEE,* vol. 61, pp. 1668–1694, Dec. 1973.

[9] C. Polk, "Optimal Fresnel-zone gain of a rectangular aperture," *IRE Trans. Antennas Propagat.*, vol. AP-4, pp. 65–69, Jan. 1956.

[10] R. H. T. Bates and J. Elliott, "The determination of the true sidelobe level of long broadside arrays from radiation-pattern measurements in the Fresnel region" *Proc. Inst. Elec. Eng. Monograph 169R,* pp. 307–312, Mar. 1956.

[11] J. Brown, "A theoretical analysis of some errors in aerial measurements," *Proc. Inst. Elec. Eng. Monograph 285R,* pp. 343–351, Feb. 1958.

[12] J. Brown and E. V. Jull, "The prediction of aerial radiation patterns from near-field measurements," *Proc. Inst. Elec. Eng.*, vol. 108B, pp. 635–644, Nov. 1961.

[13] D. M. Kerns, "Analytical techniques for the correction of near-field antenna measurements made with an arbitrary but known measuring antenna," in *Abstracts of URSI-IRE Meeting,* Washington, DC, Apr.–May 1963, pp. 6–7.

[14] ——, "Plane-wave scattering-matrix theory of antennas and antenna-antenna interactions," NBS Monograph 162, U.S. Govt. Printing Office, Washington, DC, June 1981.

[15] W. M. Leach, Jr. and D. T. Paris, "Probe-compensated near-field measurements on a cylinder," *IEEE Trans. Antennas Propagat.*, vol. AP-21, pp. 435–445, July 1973.

[16] G. V. Borgiotti, "Integral equation formulation for probe corrected far-field reconstruction from measurements on a cylinder," *IEEE Trans. Antennas Propagat.*, vol. AP-26, pp. 572–578, July 1978.

[17] A. D. Yaghjian, "Near-field antenna measurements on a cylindrical surface: A source scattering-matrix formulation," NBS Tech. Note 696, Sept. 1977.

[18] F. Jensen, "Electromagnetic near-field far-field correlations," Ph.D. dissertation, Tech. Univ. Denmark, July 1970.

[19] ——, "On the probe compensation for near-field measurements on a sphere," *AEU,* vol. 29, pp. 305–308, July–Aug. 1975.

[20] P. F. Wacker, "Near-field antenna measurements using a spherical scan: efficient data reduction with probe correction," in *Inst. Elec. Eng. Conf. Publ. 113,* Conf. Precision Electromagn. Measurements, London, July 1974, pp. 286–288.

[21] ——, "Non-planar near-field measurements: Spherical scanning," NBSIR 75-809, June 1975.

[22] L. J. Ricardi and M. L. Barrows, "A recurrence technique for expanding a function in spherical harmonics," *IEEE Trans. Comput.*, vol. C-21, pp. 583–585, June 1972.

[23] R. L. Lewis, "Highly efficient processing for near-field spherical scanning data reduction," in *Dig. IEEE Antennas Propagat. Soc. Int. Symp.*, Amherst, MA, Oct. 1976, pp. 251–254.

[24] F. H. Larsen, "Probe correction of spherical near-field measurements," *Electron. Lett.*, vol. 13, pp. 393–395, July 1977.

[25] ——, "Probe-corrected spherical near-field antenna measurements," Tech. Univ. Denmark Rep. LD36, Dec. 1980.

[26] P. J. Wood, "The prediction of antenna characteristics from spherical near-field measurements—Parts I and II, theory and experimental verification," *Marconi Rev.*, vol. 30, pp. 42–68, 117–155, 1st and 2nd Quarter 1977.

[27] A. D. Yaghjian, "Simplified approach to probe-corrected spherical near-field scanning," *Electron. Lett.*, vol. 20, pp. 195–196, Mar. 1984. (*Also in Dig. Int. Symp. Antennas Propagat.*, Boston, MA, June 1984, pp. 670–673.)

[28] R. C. Wittmann, "Probe correction in spherical near-field scanning, viewed as an ideal probe measuring an effective field," in *Dig. Int. Symp. Antennas Propagat.*, Boston, MA, June 1984, pp. 674–677.

[29] A. D. Yaghjian and R. C. Wittmann, "The receiving antenna as a linear differential operator: Application to spherical near-field scanning," *IEEE Trans. Antennas Propagat.*, vol. AP-33, pp. 1175–1185, Nov. 1985.

[30] R. C. Baird, "Antenna measurements with arbitrary probes at arbitrary distances," in *High Frequency and Microwave Field Strength Precision Measurement Seminar,* NBS Rep. 9229, May 1966.

[31] R. C. Baird, A. C. Newell, P. F. Wacker, and D. M. Kerns, "Recent experimental results in near-field antenna measurements," *Electron. Lett.*, vol. 6, pp. 349–351, May 1970.

[32] A. C. Newell and M. L. Crawford, "Planar near-field measurements on high performance array antennas," NBSIR 74-380, July 1974.

[33] A. C. Newell, *Planar Near-Field Measurements,* NBS Lecture Notes, Boulder, CO, June 1985.

[34] A. D. Yaghjian, "Upper-bound errors in far-field antenna parameters determined from planar near-field measurements, Part I: Analysis," NBS Tech. Note 667, Oct. 1975.

[35] A. C. Newell, "Upper-bound errors in far-field antenna parameters determined from planar near-field measurements, Part II: Analysis and computer simulation," NBS Short Course Notes, Boulder, CO, July 1975.

[36] E. B. Joy and D. T. Paris, "Spatial sampling and filtering in near-field measurements," *IEEE Trans. Antennas Propagat.*, vol. AP-20, pp. 253–261, May 1972. (Also see Ph.D. dissertation by E. B. Joy, Georgia Inst. Technology, 1970.)

[37] A. C. Newell, National Bureau of Standards, Boulder, CO, private communication, 1984.

[38] R. G. Sharp, "Near-field measurement facility plans at Lewis Research Center," in *NASA Conf. Pub. 2269, Pt. 2,* pp. 899–921, Dec. 1982.

[39] Y. Rahmat-Samii, V. Galindo-Israel and R. Mittra, "A plane-polar approach for far-field construction from near-field measurements," *IEEE Trans. Antennas Propagat.*, vol. AP-28, pp. 216–230, Mar. 1980.

[40] Y. Rahmat-Samii and M. S. Gatti, "Far-Field patterns of spaceborne antennas from plane-polar near-field measurements," *IEEE Trans. Antennas Propagat.*, vol. AP-33, pp. 638–648, June 1985.

[41] V. Galindo-Israel and Y. Rahmat-Samii, "A new look at Fresnel field computation using the Jacobi-Bessel series *IEEE Trans. Antennas Propagat.*, vol. AP-29, pp. 885–898, Nov. 1981.

[42] C. F. Stubenrauch, "Planar near-field scanning in polar coordinates: A feasibility study," NBS Rep. sponsor SR-723-73-80, 1980.

[43] P. F. Wacker and R. Severyns, "Near-field analysis and measurement: plane polar scanning," in *Inst. Elec. Eng. Conf. Pub. 219, Pt. 1.*, pp. 105–107, Apr. 1983.

[44] R. C. Hansen, "Measurement distance effects on low sidelobe patterns," *IEEE Trans. Antennas Propagat.*, vol. AP-32, pp. 591–594, June 1984.

[45] K. R. Grimm, "Ultralow sidelobe planar near-field measurement study," in *Proc. 1982 Antenna Applications Symposium* (RADC-TR-82-339), Hanscom AFB, MA, Jan. 1983, pp. 663–682.

[46] ——, "Optimum probe design for near-field scanning of ultralow sidelobe antennas," presented at Antenna Appl. Symp., Allerton Park, IL, Sept. 1984.

[47] A. C. Newell, M. H. Francis, D. P. Kremer and K. R. Grimm, "Results of planar near-field testing with ultralow sidelobe antennas," in *Dig. Antennas Propagat. Int. Symp.*, Vancouver, Canada, June 1985, pp. 693–698.

[48] G. K. Huddleston, "Optimum probes for near-field antenna measurements on a plane," Ph.D. dissertation, Georgia Inst. Technol., Atlanta, GA, Aug. 1978.

[49] W. T. Patton, "Phased array alignment with planar near-field scanning; or determining element excitation from planar near-field data," in *Proc. Antenna Appl. Symp.*, Univ. Illinois, Sept. 1981.

[50] D. M. Kerns, "Scattering matrix description and near-field measurements of electroacoustic transducers," *J. Acoust. Soc. Am.*, vol. 57, pp. 497–507, Feb. 1975.

[51] A. C. Newell, R. C. Baird, and P. F. Wacker, "Accurate measurement of antenna gain and polarization at reduced distances by an extrapolation technique," *IEEE Trans. Antennas Propagat.*, vol. AP-21, pp. 418–431, July 1973.

[52] D. M. Kerns, "Correction of near-field antenna measurements made with an arbitrary but known measuring antenna," *Electron. Lett.* vol. 6, pp. 346–347, May 1970.

[53] ——, "New method of gain measurement using two identical antennas," *Electron. Lett.*, pp. 348–349, May 1970.

[54] D. M. Kerns and A. C. Newell, "Determination of both polarization and power gain by a generalized 3-antenna measurement method," *Electron. Lett.*, vol. 7, pp. 68–70, Feb. 1971.

[55] D. T. Paris, W. M. Leach, Jr., and E. B. Joy, "Basic theory of probe-compensated near-field measurements," *IEEE Trans. Antennas Propagat.*, vol. AP-26, pp. 373–379, May 1978.

[56] J. Appel-Hansen, "Antenna measurements," in *The Handbook of Antenna Design, vol. 1.* London: Peregrinus, ch. 8, 1982.

[57] A. D. Yaghjian, "Efficient computation of antenna coupling and fields within the near-field region," *IEEE Trans. Antennas Propagat.*, vol.

AP-30, pp. 113–128, Jan. 1982.
[58] ——, "Equivalence of surface current and aperture field integrations for reflector antennas," *IEEE Trans. Antennas Propagat.*, vol. AP-32, pp. 1355–1358, Dec. 1984.
[59] P. M. Morse and H. Feshbach, *Methods of Theoretical Physics.* New York: McGraw-Hill, 1953, ch. 13.
[60] J. R. James and L. W. Longdon, "Prediction of arbitrary electromagnetic fields from measured data," *Alta. Freq.*, vol. 38 (special issue), pp. 286–290, May 1969.
[61] J. A. Stratton, *Electromagnetic Theory.* New York: McGraw-Hill, 1941.
[62] A. D. Yaghjian, "Approximate formulas for the far field and gain of open-ended rectangular waveguide," *IEEE Trans. Antennas Propagat.*, vol. AP-32, pp. 378–384, Apr. 1984.
[63] A. C. Newell and A. Repjar, "Results of spherical near-field measurements on narrow-beam antennas," in *Dig. of Int. Symp. Antennas Propagat.*, Stanford, CA, June 1977, pp. 382–385.
[64] C. F. Stubenrauch and A. C. Newell, "Some recent near-field antenna measurements at NBS," *Microwave J.*, vol. 23, pp. 37–42, Nov. 1980.
[65] A. D. Yaghjian, "Probe correction for near-field antenna measurements," in *Proc. Antenna Applications Symp.*, Univ. Illinois, Sept. 1984.
[66] ——, "Generalized or adjoint reciprocity relations for electroacoustic transducers," *NBS J. Res.*, vol. 79B, pp. 17–39, Jan.–June 1975.
[67] A. V. Oppenheim and R. W. Schaffer, *Digital Signal Processing.* Englewood, Cliffs, NJ: Prentice-Hall, 1975, ch. 3.
[68] A. E. Siegman, "Quasi fast Hankel transform," *Opt. Lett.*, vol. 1, pp. 13–15, July 1977.
[69] A. D. Yaghjian, "The planar near-field reconstruction approach to high-resolution remote sensing of subsurface anomalies," in *High Resolution Sensing Techniques for Slope Stability Studies,* Rep. FHWA-RD-79-32 (available through NTIS, Springfield, VA 22161), Jan. 1979, ch. 4.
[70] E. B. Joy, W. M. Leach, Jr., G. P. Rodrique, and D. T. Paris, "Applications of probe-compensated near-field measurements," *IEEE Trans. Antennas. Propagat.*, vol. AP-26, pp. 379–389, May 1978.
[71] A. Repjar, National Bureau of Standards, Boulder, CO, private communication, 1984.
[72] G. P. Rodrique, E. B. Joy, and C. P. Burns, "An investigation of the accuracy of far-field radiation patterns determined from near-field measurements," Georgia Inst. Technol. Rep., Aug. 1973.
[73] E. B. Joy, "Maximum near field measurement error specification," in *Dig. Int. Symp. Antennas Propagat.*, Stanford, CA, June 1973, pp. 390–393.
[74] E. B. Joy and A. D. Dingsor, "Computer simulation of cylindrical surface near-field measurement system errors," in *Dig. Int. Symp. Antennas Propagat.*, Seattle, WA, June 1979, pp. 565–568.
[75] W. Chang, D. Fasold, and C. P. Fischer, "A new near-field test facility for large spacecraft antennas," in *Abstracts of Nat. Radio Sci. Meet.*, Boulder, CO, Jan. 1984, p. 3.
[76] F. Jensen, "Computer simulations as a design tool in near-field testing, *Inst. Elec. Eng. Conf. Pub. 169, Pt. 1,* Nov. 1978, pp. 111–114.
[77] J. Ruze, "Antenna tolerance theory—A review," *Proc. IEEE,* vol. 54, pp. 633–640, Apr. 1966.
[78] E. B. Joy and R. E. Wilson, "A simplified technique for probe position error compensation in planar surface near-field measurements," in *Proc. AMTA Meet.*, Mexico State Univ., Oct. 1982, pp. 12-1–12-10.
[79] L. E. Corey and E. B. Joy, "On computation of electromagnetic fields on planar surfaces from fields specified on nearby surfaces," *IEEE Trans. Antennas Propagat.*, vol. AP-29, pp. 402–404, Mar. 1981.
[80] M. A. Dinallo, "Extension of plane-wave scattering matrix theory of antenna-antenna interactions to three antennas: A near-field radar cross section concept," in *Proc. Antenna Appl. Symp.*, Univ. Illinois, Sept. 1984.
[81] P. J. Napier, "Reconstruction of radiating sources," Ph.D. dissertation, Univ. Canterbury, Christchurch, New Zealand, ch. 4, 1971.
[82] M. L. Crawford, "Calibration of broadbeam antennas using planar near-field measurements," in *Dig. Conf. Precision Electromagn. Measurements,* Boulder, CO, pp. 53–56, June–July 1976.
[83] A. G. Repjar and D. P. Kremer, "Accurate evaluation of a millimeter wave compact range using planar near-field scanning," *IEEE Trans. Antennas Propagat.*, vol. AP-30, pp. 419–425, May 1982.
[84] W. H. Kummer and E. S. Gillespie, "Antenna measurements—1978," *Proc. IEEE,* vol. 66, pp. 483–507, Apr. 1978.
[85] N. J. Gamara, "Pattern predictability on the basis of aperture phase and amplitude distribution measurements," Electron. Defense Lab., Mountain View, CA, Tech. Memo. EDL-M247, ASTIA Doc. AD 236298, Mar. 1960.

Arthur D. Yaghjian (S'68–M'69–SM'84), for a photograph and biography please see page 5 of the January 1984 issue of this TRANSACTIONS.